



## SMALL TARGET DETECTION BASED ON INFRARED IMAGE ADAPTIVE

Hao Chen, Hong Zhang, Yifan Yang and Ding Yuan  
Image Processing Center, Beihang University, Beijing 100191, China  
Email: chenhaoyiyou@sa.buaa.edu.cn

---

*Submitted: Oct. 26, 2014*

*Accepted: Jan. 23, 2015*

*Published: Mar. 1, 2015*

---

*Abstract- This paper studies the multi-resolution analysis of infrared image preprocessing method based on wavelet transform, wavelet transform infrared image of small target for pretreatment, after pretreatment suppressed image background clutter, improved signal to noise ratio. On this basis, studies based on infrared image sequences generated background Kalman filter and target detection algorithm, given the principle of the algorithm, time-domain method for generating fading background and moving object extraction methods such as recursive least squares method, and the experimental results show that the algorithm capable of detecting small targets in infrared images, with good results. based pretreatment small target motion continuity characteristics studied image sequences small moving target detection algorithm based on weighted dynamic programming, dynamic programming algorithm principle is given, analysis of the direct method and the accumulation of gray dynamic programming algorithm based on similar likelihood function for dynamic programming problems arise energy diffusion gives improved dynamic programming algorithm: weighted dynamic programming algorithm, the algorithm implementation steps, testing and experimental structure the results were analyzed, the results show that the algorithm for small moving target detection with good results. Finally, this paper studied the infrared image reject false target trajectory get the real target trajectory correlation method, so as to improve the detection rate and reduce the false alarm rate the purpose.*

**Index terms:** Target enhancement, local spectrum suppression, regular patches, log amplitude spectrum, TDI.

## I. INTRODUCTION

The infrared imaging guidance system as a complete system composed of several modules, generally can be divided into: moving target detection, target recognition, target acquisition, target tracking is finally to the point of attack for confirmation [1, 2]. Moving object detection as a module initial guidance system is the key of the whole system, infrared technology can remote imaging characteristics so often has small moving targets in infrared images obtained, the small moving target detection in infrared image has gradually become one of the important symbols of modern military system, intelligent [3-6]. Infrared image of the moving small target imaging area is generally much smaller, in the image of complex background, the target is also very likely by the amount of noise, often have low SNR image, these adverse factors make the detection performance of infrared images of small moving target detection method is difficult to be guaranteed [7-11].

Wavelet transform is a new image processing technology has been more and more attention [12]. The background distribution area in infrared images often present large and continuous distributions, grey space distribution of infrared image has more relevance, can be regarded as a kind of slow change and it is a 2D nonstationary random process. The radiation intensity of background radiation intensity in the image is often lower than the target, there is no correlation between radiation intensity of both, so you can think of the background in the low-frequency part of the image, the target is in the high frequency part of image, and the analysis of multi resolution wavelet transform technique can be on the low frequency and high frequency part of the image in the separate analysis and processing, background noise suppression in the low frequency part, enhanced in high frequency part of the goal, to achieve the goal of improving the signal-to-noise ratio, which lay a foundation for the detection of small target. Based on the PFT, the Phase Spectrum of Quaternion Fourier Transform (PQFT) [13] was later proposed by using the quaternion Fourier Transform. With the development of saliency estimation techniques, the visual attention mechanism has been adopted to detect the infrared targets [14], but it is still very challenging to achieve an accurate target detection result when handling the infrared image containing the comparably dim targets. Motivated by the above difficulties, we adopt the idea of local spectrum suppression and propose a novel method to enhance the infrared small target effectively. Specifically, we first compute the log amplitude spectrum of an input infrared image,

and locate the spikes in the log amplitude spectrum by using the cubic facet model. The spikes are then suppressed via the local spectrum filtering in the frequency domain.

## II. SPARSE REPRESENTATION OF IMAGE THEORY

### 2.1 The research status

Small target detection algorithm based on time domain, usually by utilizing the continuity between adjacent frames of small target motion trajectory to gradually eliminate false target, determine the true goal, the basic process is generally the first on a frame infrared image noise reduction, some suspicious position determines the existence of small target, and according to the direction of movement of the small target and the motion speed and other information, prediction of all position the next frame of infrared small target in image appear; after the next frame infrared image noise reduction, determine the number of suspected location exists small target in the frame, make the comparison of prediction results and a frame, and the prediction of small and medium frame infrared image target next possible after all the position predicted and compared several frame image, false target gradually excluded, motion trajectory of the true target gradually determine. The advantage of this method is that can make full use of multi frame contained in infrared image information, which greatly improves the detection probability of infrared image, even if the output signal-to-noise ratio is very low, the detection probability of small target is relatively high; the disadvantage is the unknown motion characteristics when the small target, the need for prediction, in all cases the workload great, the algorithm efficiency is low.

At present the main study of small target detection based on time domain: in 1988, Reed et al proposed by three-dimensional matching filter method to detect moving targets, in determining the target trajectory and determine the target position of each frame image in [15]. In 1995, Choi et al for the target in the 3-D space trajectory projection onto a plane problems are studied, and some suggestions are put forward to forecast the target position prediction and detection, and compared directly in 3D space, the efficiency of the algorithm greatly improved [16]. In 2010, Yuan Weicai et al proposed a target detection algorithm based on inter frame difference between adjacent frames, with characteristics of background changes very little and the goal of continuous motion, obtained the two adjacent frame difference to distinguish the background part and a

target in the image, the algorithm implementation is very simple, but when the target is very small, the goal difference results are easily mistaken for noise [17].

## 2.2 The basic principle of sparse representation

The number of vector elements contained called vector dimension, a M dimensional vector by M elements, each element of the vector corresponds to the value of the dimensions, namely  $\varphi = \{\varphi_i\}, i = 1, 2, \dots, M$  . T linearly independent vectors  $\Psi = \{\varphi_i\}, i = 1, 2, \dots, T$  , can be composed of a set of base, can use linear combinations of them represent other vector in this space. For any M dimensional vector space, when  $T < M$ , the linear combination can only a part of the representation of space vector, now called this group basis is underdetermined, or also called incomplete. But when  $T = M$ , any vector s M dimensional vector space can only use linear combinations to represent:

$$s = \sum_i a_i \varphi_i, i = 1, 2, \dots, M \quad (1)$$

Because of the infinite matrix is full rank, so any vector s in only carries on the decomposition, are uniquely determined factorization results obtained. Usually the type (2) written in matrix form:

$$s = [\varphi_1 \quad \varphi_2 \quad \dots \quad \varphi_M] \begin{bmatrix} a_1 \\ a_2 \\ \vdots \\ a_M \end{bmatrix} = \Psi a \quad (2)$$

## 2.3 The theory of wavelet analysis

Wavelet analysis of the rise gradually in recent years and better solve the first limitation of complete orthogonal basis expansion, it can provide the local resolution is better. Based on the basic thought of the traditional Fourier transform, wavelet analysis is introduced to all basis functions with good attenuation characteristic in time domain and frequency domain, time domain and frequency domain to achieve resolution compromise, it is seen as more than half a century of harmonic analysis work in the field, has been widely used in the field of science and technology of image processing, computer vision, pattern recognition, speech recognition [18, 19]. "Wavelet", as the name suggests is a small region, finite length, mean 0 waveforms, so use the term "wavelet transform" on behalf of the mathematical waveform [20]. In fact, the wavelet is

an alternate oscillation, and the waveform is attenuated, and DC component of the oscillating wave zero. The wavelet transform is the same as Fourier transform is decomposed in the orthogonal basis, and Fourier different is that you can choose different orthogonal bases, and then through the translation and scaling decomposition [21, 22]. The wavelet function is defined:

Let it change for the bubble, if meet the formula full weight

$$\int_R \frac{|\hat{\psi}(\omega)|^2}{\omega} d\omega < \infty \tag{3}$$

According to the formula (5) for dilation and translation of the basic wavelet, telescopic translation after a wavelet series  $\psi_{a,b}(t)$ :

$$\psi_{a,b}(t) = \frac{1}{\sqrt{|a|}} \psi\left(\frac{t-b}{a}\right) \quad a, b \in R, a \neq 0 \tag{4}$$

The definition of Daubechies series wavelet basis for:

$$p(y) = \sum_{k=0}^{N-1} C_k^{N-1+k} y^k \tag{5}$$

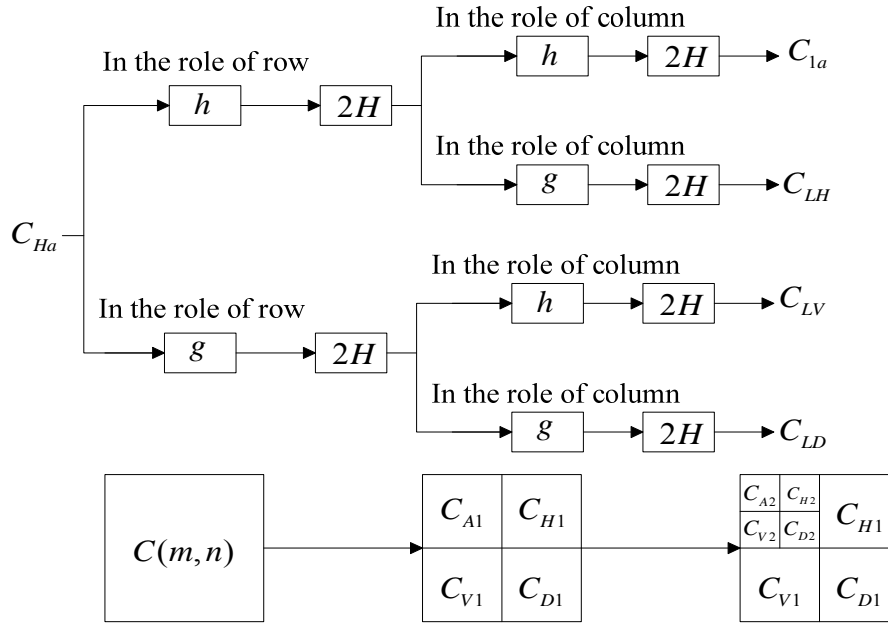
Where C is the binomial coefficient, so:

$$|m_0(w)|^2 = (\cos^2(\frac{w}{2}))^N p(\sin^2(\frac{w}{2})) \tag{6}$$

At the same time to meet:

$$m_0(w) = \frac{1}{\sqrt{2}} \sum_{n=0}^{2N-1} h_n e^{-inw} \tag{7}$$

Scaling function and wavelet function, Daubechies wavelet series is determined by the coefficient of C.



Two wavelet decomposition diagram

Figure 1. The first wavelet transform

Figure 1 showed after the first wavelet transform, the original image is decomposed into 4 coefficient matrix, and each coefficient matrix for the original image resolution 1/4: low frequency (approximate) coefficient  $C_{A1}$ , horizontal detail coefficient  $C_{H1}$ , vertical detail coefficients  $C_{V1}$ , diagonal detail coefficients  $C_{D1}$ . The second decomposition will be  $C_{A1}$  for the original image, the coefficient matrix again divided into 4 smaller, 1/16 each of the coefficient matrix of the original image resolution.

### III. ADAPTIVE INFRARED SMALL TARGET DETECTION FOR OVER COMPLETE SPARSE REPRESENTATION OF IMAGE

#### 3.1 The infrared small target image model

Given a digital infrared image  $f(x, y)$  of size  $M \times N$ , its transformed form in the frequency domain is:

$$F(u, v) = \frac{1}{MN} \sum_{x=0}^{M-1} \sum_{y=0}^{N-1} f(x, y) \exp(-j2\pi(ux/M + vy/N)) \quad (8)$$

As in the 1-D case, (2) must be the evaluated values of the discrete variables  $u$  and  $v$  in the ranges  $u = 0, 1, 2, \dots, M-1$  and  $v = 0, 1, 2, \dots, N-1$ . Given the transform  $F(u, v)$ ,  $f(x, y)$  can be obtained by using the inverse discrete Fourier transform:

$$f(x, y) = \frac{1}{MN} \sum_{u=0}^{M-1} \sum_{v=0}^{N-1} F(u, v) \exp(j2\pi(ux/M + vy/N)) \quad (9)$$

In general, the components of the Fourier transform are complex quantities. As in the analysis of complex numbers, it is more convenient to express  $F(u, v)$  in polar coordinates:

$$F(u, v) = |A(u, v)| \exp(-jP(u, v)) \quad (10)$$

where its magnitude  $A(u, v)$ , named the amplitude spectrum of the Fourier transform, can be expressed by,

$$A(u, v) = [R^2(u, v) + I^2(u, v)]^{1/2} \quad (11)$$

And  $P(u, v)$ , called the phase spectrum of the transform, is defined as,

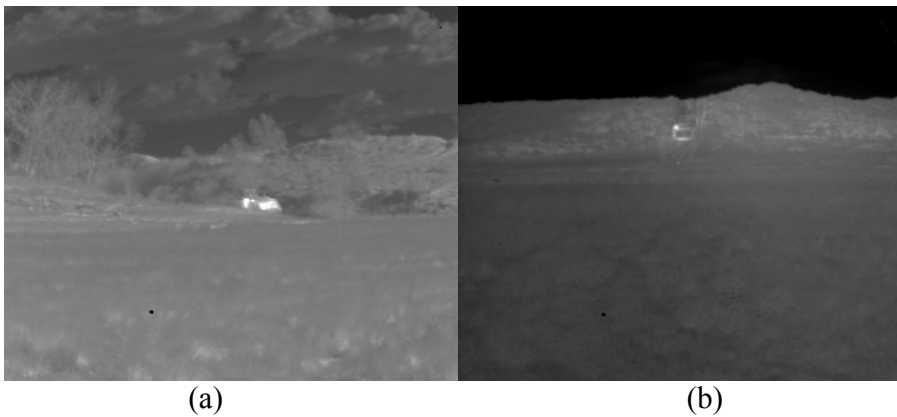
$$P(u, v) = \arctan \left[ \frac{I(u, v)}{R(u, v)} \right] \quad (12)$$

Both  $A(u, v)$  and  $P(u, v)$  are the real and imaginary parts of  $F(u, v)$  respectively.

Because the zero-frequency term dominates the values of the amplitude spectrum, the dynamic range of other intensities in the displayed image are compressed. To bring out those details, we perform a log transformation. The log amplitude spectrum is obtained by:

$$L(u, v) = \log(A(u, v)) \quad (13)$$

For a better illustration of the above amplitude spectrum, Figure 2 (a) shows an original infrared image. Figure 2 (b) shows the amplitude spectrum and Figure 2 (d) shows its corresponding 3D mesh view. Figure 4 (c) shows the log amplitude spectrum.



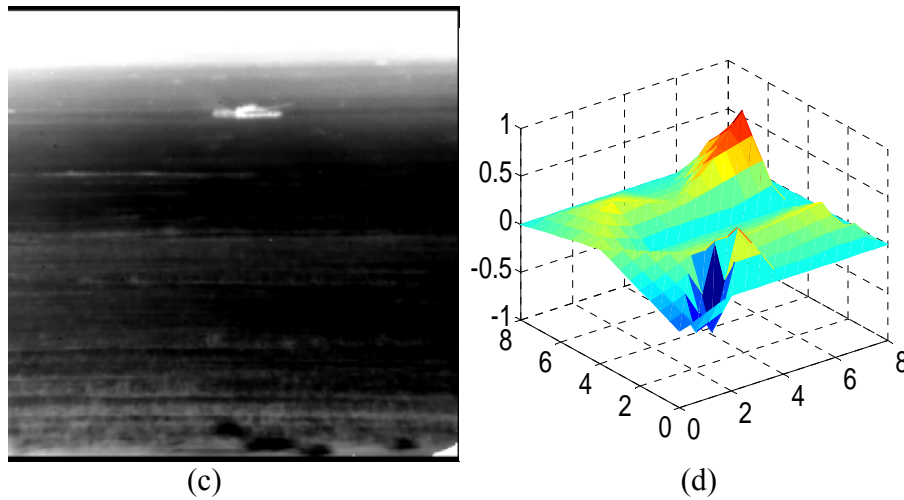


Figure 2. The original infrared image and its log amplitude spectrum. (a) The infrared image; (b) the amplitude spectrum; (b) The log amplitude spectrum; (d) The 3D mesh view of the amplitude

Before and after treatment changes the performance indicators such as shown in table 1:

Table 1. Comparison of average filter performance index comparison

Performance index	Original	Results figure(3×3)	Results figure(5×5)	Results figure(7×7)
Contrast	1.41535	2.8125	3.9763	3.4692
SNR	2.8543	3.1543	5.1645	4.7538
MSE	183.375	128.765	102.432	113.785

Comparison of average filter does not depend on any prior knowledge, only is the evaluation of the image features and existing information, the proposed method, has good effect on eliminating the high frequency noise. From the changes of the experimental results and performance indicators can be seen, the local window closer to the target size, the filtering effect is better, but the amount of calculation will be as the linear increase; at the same time is not easy to control, because of not considering the specific effects of noise, the noise can not automatically according to the change of spot and automatically adjust the size of the filtering window, namely adaptive relatively poor.

### 3.2 Log Amplitude Spectrum Calculation

The endpoint detection is from a section of speech signal in the detection of the starting point and ending point of speech, delete the silent section, in order to reduce the calculation amount of feature extraction and accuracy, shorten the training and recognition time system, improve the recognition rate. The traditional endpoint detection method is the use of image signal short-time

energy and short-time zero crossing rate to achieve, this is because of the short time energy point of view, the maximum imaged signal, sound signal of silent period, the minimum; from the zero crossing rate, imaged signal of the lowest, in silence, the sound signal.

Suppose a image over frame processing after the N frame signal for  $X_n(m)$ , its length is denoted by N, is defined by short-time energy and short-time zero crossing rate are as follows:

Short-time energy  $E_n$ :

$$E_n = \sum_{m=0}^{N-1} x_n^2(m)$$

The short-time zero crossing rate of  $Z_n$ :

$$Z_n = \frac{1}{2N} \sum_{m=0}^{N-1} |\text{sgn}[x_n(m)] - \text{sgn}[x_n(m-1)]| \tag{14}$$

$\text{Sgn}[]$  is the sign function, the expression for the:

$$\text{sgn}(x) = \begin{cases} 1, & x \geq 0 \\ -1, & x < 0 \end{cases} \tag{15}$$

Figure 3 shows a section of imaged signal and the image signal short-time energy and short-time zero crossing rate:

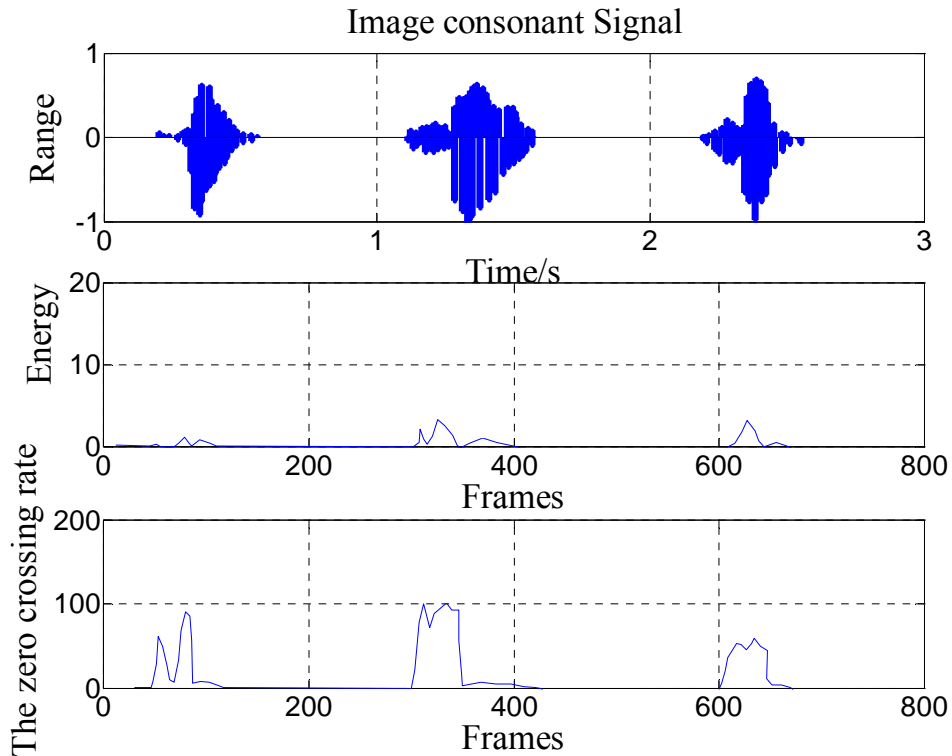


Figure 3. Section of imaged signal and the image signal short-time energy

The approximate fitting problem is to determine coefficients  $a_0, a_1, \dots, a_K, K \leq N-1$  such that

$$e^2 = \sum_{(r,c) \in S} \left[ d(r,c) - \sum_{n=0}^K a_n P_n(r,c) \right]^2 \quad (16)$$

is minimized. In either case the result is

$$a_m = \frac{\sum_{(r,c) \in S} P_m(r,c) d(r,c)}{\sum_{(r,c) \in S} P_m^2(r,c)} \quad (17)$$

The exact fitting coefficients and the least squares coefficients are identical for  $m=0,1,\dots,K$ . Each fitting coefficient  $a_m$  can be computed as a linear combination of the data values. For each index  $(r,c) \in S$ , the data value  $d(r,c)$  is multiplied by the weight  $w_m$ :

$$w_m = \frac{\sum_{(r,c) \in S} P_m(r,c)}{\sum_{(r,c) \in S} P_m^2(r,c)} \quad (18)$$

which is an appropriate normalization of an evaluation of polynomial  $P_m(r,c)$  at index  $(r,c)$ .

Figure 5 shows the examples of weights for a  $3 \times 3$  neighborhood.

Clean image and noise simulation mixed through 8 stage hybrid filter, mixed filter:

$$H = \begin{bmatrix} h_{11} & h_{12} \\ h_{21} & h_{22} \end{bmatrix} \quad (19)$$

$$h_{11} = [0.1 \quad 0.55 - 0.43 \quad 0.73 \quad 0.26 - 0.38 \quad 0.12 \quad 0.75]$$

$$h_{21} = [0.28 - 0.14 \quad 0.54 - 0.34 \quad 0.19 \quad 0.25 \quad 0.62 \quad 0.48]$$

$$h_{22} = [0.41 \quad 0.12 \quad 0.36 - 0.87 \quad 0.71 \quad 0.95 - 0.33 \quad 0.44] \quad (20)$$

### 3.3 The steps of small target detection algorithm

In order to enhance infrared small targets, it is necessary to suppress the sharp spikes which lead to regular patches. In the frequency domain, the regions  $S_i (i=1,2,3,\dots)$  which contain the sharp spikes of the log amplitude spectrum  $L(u,v)$  have to be discriminated firstly by using the cubic facet model, and then the rest regions are called region B. Consequently, the traditional log amplitude spectrum can be formulated as:

$$L(u,v) = B + \sum_{i=1}^n S_i \quad (21)$$

Then, the spikes can be suppressed by convoluting  $S_i$ :

$$S_i' = S_i * h_n(f) \quad (22)$$

where  $h_n(f)$  is an  $n \times n$  matrix and defined by:

$$h_n(f) = \frac{1}{n^2} \begin{pmatrix} 1 & 1 & \cdots & 1 \\ 1 & 1 & \cdots & 1 \\ \vdots & \vdots & \ddots & \vdots \\ 1 & 1 & \cdots & 1 \end{pmatrix} \quad (23)$$

It is necessary to explain the setting of parameter  $n$  in (17). According to [16], the averaged curve indicates a local linearity. Therefore, it is reasonable to adopt a local average filter  $h_n(f)$  to approximate the shape of the log amplitude spectrum. Any variation of the size of  $h_n(f)$  only has slight effect on the results. And the smaller value the  $n$  is set, the more efficient the algorithm is. Our experiments show that  $n = 3$  is a good compromise to achieve a good result.

Substituting (16) with (17), the filtered log amplitude spectrum is then rewritten as,

$$L(u, v) = B + \sum_{i=1}^n S_i' \quad (24)$$

Based on the above discussion, we define the enhanced map  $g(x, y)$  hereafter as:

$$g(x, y) = F^{-1}\{L(u, v)e^{iP(u, v)}\} \quad (25)$$

### 3.4 The Whole Method of Small Target Enhancement

Figure 4 shows the diagram illustrating our novel infrared small target enhancement method. In the first step, we calculate the amplitude spectrum and phase spectrum of the infrared image. Because the zero-frequency term dominates the values of the amplitude spectrum, the dynamic range of other intensities in the displayed image are compressed. To bring out those details, we adopt the log amplitude spectrum representation  $L(u, v)$ .

In the second step, the sharp spikes are located in the log amplitude spectrum by using the cubic facet model. The cubic facet model assumes that in each neighborhood, the underlying grey-level intensity surface can be approximated by a cubic function. We define the 2D discrete orthogonal polynomials and show 9 sample masks for the  $3 \times 3$  window.

In the third step, unlike recent approaches by using global spectral filtering, we define the concept of local spectrum suppression which adopts local spectrum filtering to smooth the spikes in the amplitude spectrum, thereby producing the pop-out of the infrared targets. In this work only the amplitudes are involved in the convolution while the phase information remains in the frequency domain.

Finally, the target enhancement result in the spatial domain is obtained by reconstructing the 2D signal using the original phase and the filtered log amplitude spectrum. It could be observed that non-salient parts (including uniform parts) are well suppressed by using the local spectrum suppression.

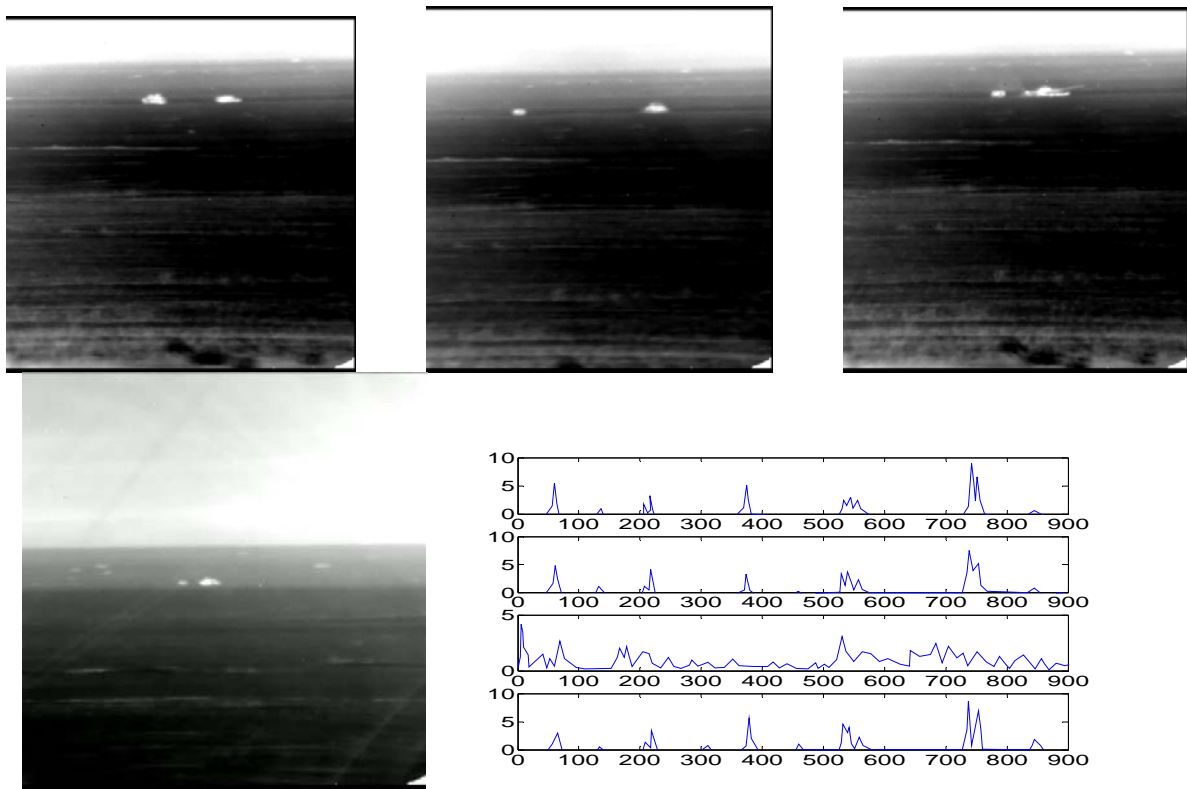


Figure 4 The overview of the proposed method in this paper

#### IV. EXPERIMENTAL RESULTS AND ANALYSIS

The following figure shows the different SNR conditions generated with a small target infrared image of the original, pay attention to the map positions of the small target and attenuation parameters is a random: Infrared small target image containing noise generated at different SNR was shown in Figure 5. Figure 6 was the original images and their enhanced maps.

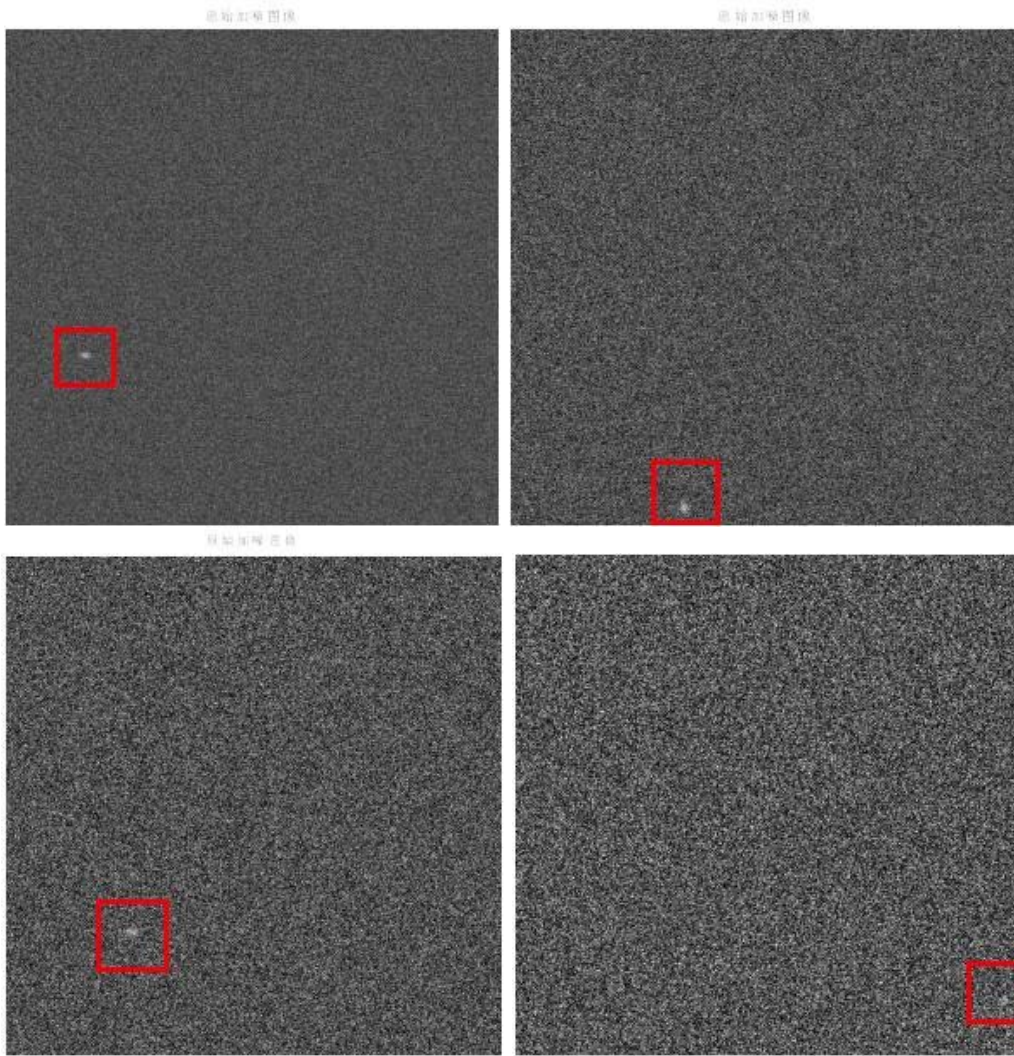
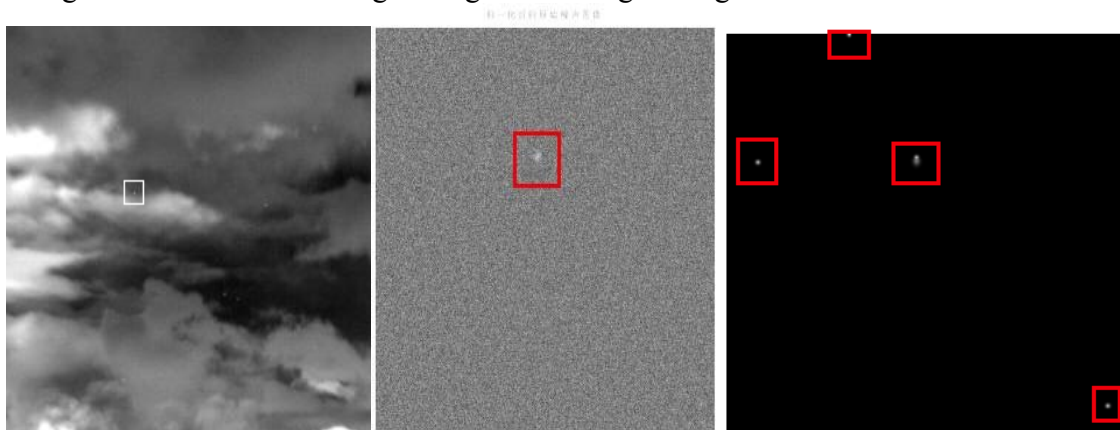


Figure 5. Infrared small target image containing noise generated at different SNR



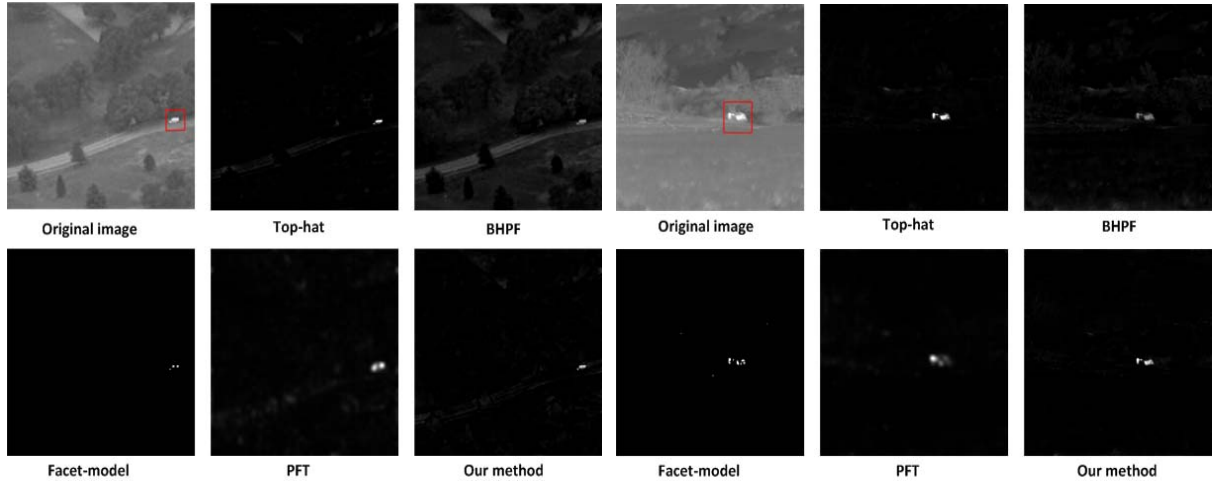


Figure 6 The original images and their enhanced maps

In practical application, the threshold value of line can be obtained by the experiment or experience. In this paper, the line value is 0.05. When containing only a small target in the original image, if the final test result in much of sub image blocks are detected in the small target, usually because of the threshold line is too small, the emergence of false alarm, but the actual situation is not always so.

For fair a further comparison quantitatively, two common evaluation indicators [19], i.e., signal-to-clutter ratio gain (SCR) and background suppression factor (BSF), are defined as follows:

$$SCR = \frac{|\mu_t - \mu_b|}{\sigma_b} \quad (26)$$

where  $\mu_t$  is the average pixel value of the target,  $\mu_b$  and  $\sigma_b$  are the average pixel value and the standard deviation of the pixel values in neighboring area around the target, respectively.

$$BSF = \frac{C_{in}}{C_{out}} \quad (27)$$

where  $C$  is calculated as the standard deviation of background. The subscripts *in* and *out* express the images before and after the detection. Because the small target size varies within a range, we use a variable neighboring area with respect to the target. As shown in Figure 9, if the size of a small target is  $a \times b$ , the size of its background rectangle is  $(a + 2d) \times (b + 2d)$ ,  $d$  is a constant which equals to 20 pixels in this paper. The algorithm flow chart to predict tracker was shown in Figure 7.

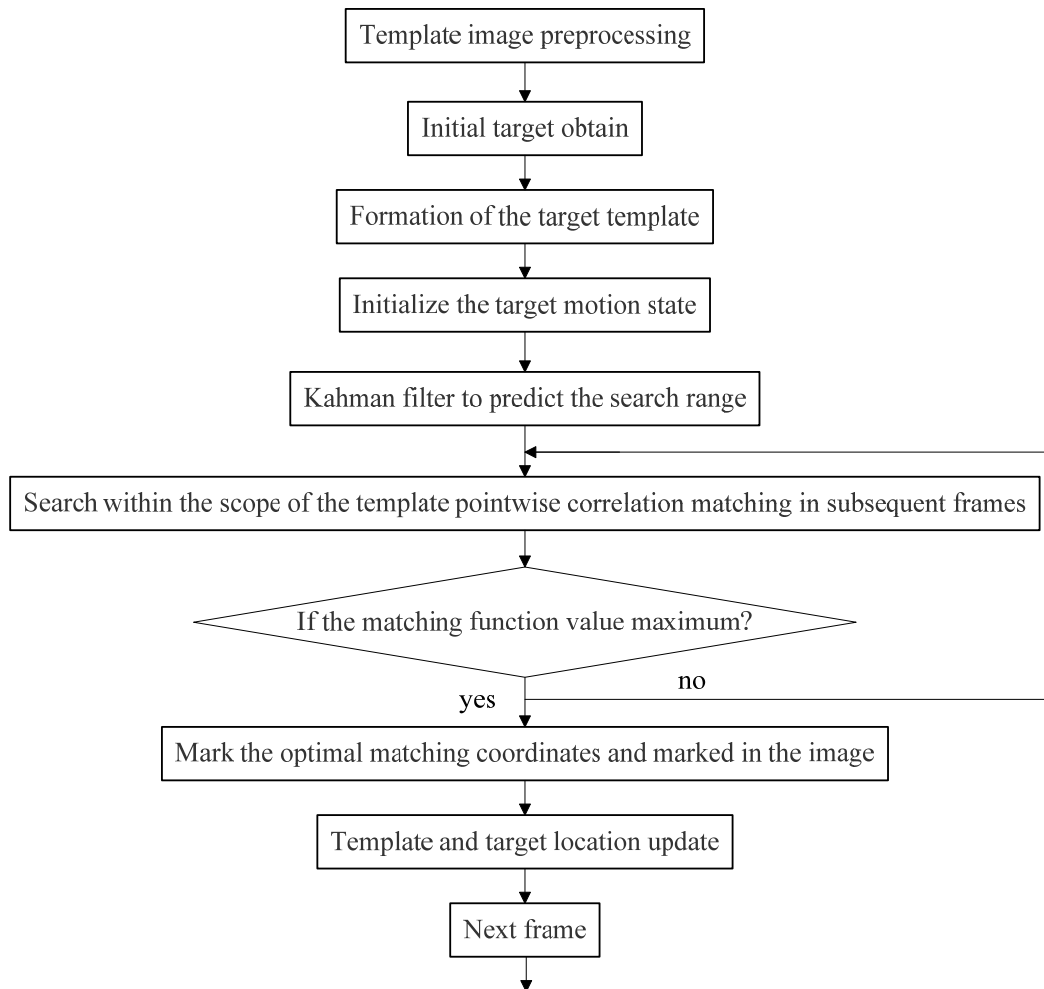


Figure 7 The target and background model

Experiments are implemented by *Matlab-2013a* software on a PC with the Intel (R) Core (TM) i5-2400 CPU. The run-time of each method for the images is recorded.

Gauss gray model was first proposed by Chan, the simple point source target using two-dimensional Gauss distribution, the mathematical formula for the:

$$I(i, j) = I_m \exp\left(-\frac{1}{2} \left[ \frac{(i-x_0)^2}{\sigma_x^2} + \frac{(j-y_0)^2}{\sigma_y^2} \right]\right) \quad (28)$$

In the formula,  $I_m$  is the maximum gray value at the center of the target, the maximum brightness decided target;  $\sigma_x$  and  $\sigma_y$  levels were attenuation parameters and vertical attenuation parameters, determines the target pixel value attenuation characteristics;  $(x_0, Y_0)$  the center position for the target in infrared image;  $(i, j)$  to coordinate the value of each pixel in infrared image. The figure below shows the use of Gauss gray model. The pixel near infrared small target

model and the center of the generated values, where  $I_m=100$ ,  $\sigma_x$  and  $\sigma_y$  were 0.5, 0.5. Table 2 showed the value of gray scale image center

Table 2. The value of gray scale image center

5.2382e-10	2.1324e-7	1.6321e-6	2.1324e-7	5.2382e-10
1.3362e-05	0.0058	0.0326	0.0058	1.3362e-05
0.0058	1.6257	12.3548	1.6257	0.0058
0.0326	12.3548	100	12.3548	0.0326
0.0058	1.6257	12.3548	1.6257	0.0058
1.3362e-05	0.0058	0.0326	0.0058	1.3362e-05
5.2382e-10	2.1324e-7	1.6321e-6	2.1324e-7	5.2382e-10

From the graph we can easily see that Gauss gray model shortcomings: attenuation is too sharp, causing the target edge presents a saw tooth shape, but the actual imaging infrared small target is generally relatively smooth edge. Therefore, the need for Gauss gray level attenuation model parameters and vertical attenuation  $\sigma_x$  and  $\sigma_y$  respectively to make the corresponding constraint, when  $I_m$  is large,  $X$  and  $\sigma_y$  should also take larger values, when  $I_m$  is low,  $X$  and the  $\sigma_y$  should also take a small value. the ratio of  $I_m$  and  $X$  and  $\sigma_y$  within a certain range, which is the improved Gauss gray model:

$$I(i, j) = I_m \exp\left(-\frac{1}{2} \left[ \frac{(i-x_0)^2}{\sigma_x^2} + \frac{(j-y_0)^2}{\sigma_y^2} \right]\right) st \begin{cases} T_1 \leq \frac{I_m}{\sigma_x} \leq T_2 \\ T_1 \leq \frac{I_m}{\sigma_y} \leq T_2 \end{cases} \quad (29)$$

The value of the constraint parameter  $T_1$  and  $T_2$  decided by experience. The figure below shows the pixel near infrared small target model and center Gauss gray model generated using the improved value, including  $I_m=100$ ,  $X$  and the  $Y$  were 0.5, 0.5,  $T_1=20$ ,  $T_2=60$ .

The value of the constraint parameter  $T_1$  and  $T_2$  decided by experience. The figure below shows the pixel near infrared small target model and center Gauss gray model generated using the improved value, including  $I_m=100$ ,  $X$  and the  $Y$  were 0.5, 0.5,  $T_1=20$ ,  $T_2=60$ . Table 3 showed the value of constraint gray scale image center

Table 2: The value of constraint gray scale image center

73.2367	78.8303	79.5432	78.8303	73.2367
82.5428	87.1628	90.0216	87.1628	82.5428
87.8943	96.7453	98.2342	96.7453	87.8943
92.6552	98.3264	100	98.3264	92.6552
87.8943	96.7453	98.2342	96.7453	87.8943
82.5428	87.1628	90.0216	87.1628	82.5428
73.2367	78.8303	79.5432	78.8303	73.2367

Obviously, with Gauss gray model improved, infrared target edge re generate the smoother, more consistent with the actual target.

## V. CONCLUSION

Accurate detection of small infrared target for precision guide weapons early target acquisition, target tracking has important significance, is the key to realize intelligent and automated guided weapons. Restricted by various factors, the infrared image of COSCO at infrared imaging generated goals are often very weak, occupy the area may be only several or more than ten pixels cannot be extracted from the target shape and texture information, and by the background complexity and atmospheric disturbance and other factors, the image often contains more clutter and the noise, so that the target submerged in which it is difficult to distinguish, this pair of infrared small target detection difficulties. For the general steps of infrared small target detection is the first of the infrared image preprocessing, and then rely on multi frame detection image sequence continuity. This paper studies the infrared image preprocessing algorithm, correlation algorithm for multi frame detection.

## VI. REFERENCES

- [1] Lian Zhao, Mark, J.W., Integrated Power control and rate allocation for radio resource management in uplink wideband CDMA systems, Sixth IEEE International Symposium on a World of Wireless Mobile and Multimedia Networks, pp.428-436, 2005.
- [2] Qi S X, Ma J, Li H, Zhang S, et al. Infrared small target enhancement via phase spectrum of Quaternion Fourier Transform, Infrared Physics & Technology, vol.62, pp.50-58, 2014.

- [3] Aparna Akula; et al., Adaptive Contour-Based Statistical Background Subtraction Method for Moving Target Detection in Infrared Video Sequences, *Infrared Physics & Technology*, vol. 63, pp.103–109, 2014..
- [4] Qi Yang; Junwei Wang; Zhirong Liu; Feng Bao, Application of Median Filtering on Piv Images Analysis, 2011 International Conference on ter Science and Service System (CSSS), pp. 2108-2111, 2011 .
- [5] Peng, Guihua; Chen, He; Wu, Qiang, Infrared Small Target Detection Under Complex Background, *Advanced Materials Research*, vol.346, pp.615-619, 2012.
- [6] Gang Cao Yao Zhao Rongrong Ni Lifang Yu Huawei Tian, Forensic Detection of Median Filtering in Digital Images, 2010 IEEE International Conference on Multimedia and Expo (ICME), pp.89 - 94, 2010 .
- [7] Wang X, Liu L, Tang ZM. Infrared dim target detection based on fractal dimension and third-order characterization. *Chinese Optics Letters*, vol.7, no.10, pp.931-933, 2009.
- [8] Jufeng Zhao, Huajun Feng, et al., Real-time automatic small target detection using saliency extraction and morphological theory, *Optics & Laser Technology*, vol.47, pp.268–277, 2013..
- [9] Itti L, Koch C, Niebur E. A model of saliency-based visual attention for rapid scene analysis, *IEEE Trans. Pattern Anal. Mach. Intell*, vol.20, no. 12, pp.1254-1259, 1998.
- [10] Ko B C, Nam J. Object-of-interest image segmentation based on human attention and semantic region clustering, *J. Opt. Soc. Am. A*, vol.23, pp. 2462-2470, 2006.
- [11] Xu Y, Zhao Y, Jin C, et al. Salient target detection based on pseudo-Wigner-Ville distribution and Renyi entropy, *Opt. Lett.*, 35, 475-477, 2010.
- [12] Li W. Saliency-based automatic target detection in forward looking infrared images, 2009 16th IEEE International Conference on Image Processing (ICIP), pp. 957-960, 2009.
- [13] Li J, An X, Xu X, et al. Visual saliency based on scale-space analysis in the frequency domain. *IEEE Trans. Pattern Anal. Mach. Intell*, vol.35, no. 4, pp. 996-1010, 2013.
- [14] Haralick M. Digital step edges from zero crossing of second directional derivatives. *IEEE Trans. Pattern Anal. Mach. Intell*, Vol.6, pp. 58-68, 1984.
- [15] Yang L, Yang J, Yang K. Adaptive detection for infrared small target under sea-sky complex background, *Electron. Lett.* 40 (17) (2004) 1083-1085.

- [16] Wang G D, Chen C Y, Shen X B. Facet-based infrared small target detection method, *Electron. Lett*, vol.41, no. 22, pp.1244-1246, 2005.
- [17] Hou X, Zhang L. Saliency Detection: A Spectral Residual Approach, *IEEE Conference on Computer Vision and Pattern Recognition*, pp. 1 – 8, 2007.
- [18] Guo C, Ma Q, Zhang L. Spatio-Temporal Saliency Detection Using Phase Spectrum of Quaternion Fourier Transform, *IEEE Conference on Computer Vision and Pattern Recognition*, pp. 1 – 8, 2008.
- [19] Duncan J, Humphreys G. Visual Search and Stimulus Similarity, *Psychological Rev.*, vol. 96, no. 3, pp. 433-458, 1989.
- [20] G. Sen Gupta, S.C. Mukhopadhyay and M Finnie, Wi-Fi Based Control of a Robotic Arm with Remote Vision, *Proceedings of 2009 IEEE I2MTC Conference, Singapore, May 5-7, 2009*, pp. 557-562.
- [21] Qi S X, Ma J, Tao C, et al. A robust directional saliency-based method for infrared small-target detection under various complex backgrounds. *IEEE Geoscience and Remote Sensing Letters*, vol.10 , pp. 495-499, 2013.
- [22] G.Sengupta, T.A.Win, C.Messom, S.Demidenko and S.C.Mukhopadhyay, “Defect analysis of grit-blasted or spray printed surface using vision sensing technique”, *Proceedings of Image and Vision Computing NZ, Nov. 26-28, 2003, Palmerston North*, pp. 18-23.
- [23] Alfredo Vacearo, Domenico Villacei. Performance analysis of low earth orbit satellites for Power system communication, *Electric Power Systems Research*, vol.73, no.3, pp. 287-294, 2005.
- [24] Yanmin LUO, Peizhong LIU and Minghong LIAO, An artificial immune network clustering algorithm for mangroves remote sensing image, *International Journal on Smart Sensing and Intelligent Systems*, VOL. 7, NO. 1, pp. 116 – 134, 2014